


FULL PAPER

Open Access



Homogeneity and heterogeneity in near-infrared FTIR spectra of Ryugu returned samples

Kentaro Hatakeda^{1,2*} , Toru Yada¹, Masanao Abe^{1,3}, Tatsuaki Okada^{1,4}, Aiko Nakato¹, Kasumi Yogata¹, Akiko Miyazaki¹, Kazuya Kumagai^{1,2}, Masahiro Nishimura¹, Yuya Hitomi¹, Hiromichi Soejima^{1,2}, Kana Nagashima¹, Miwa Yoshitake¹, Ayako Iwamae¹, Shizuho Furuya¹, Tomohiro Usui^{1,4} and Kohei Kitazato⁵

Abstract

Surface and subsurface materials of C-type near-Earth asteroid 162173 Ryugu were collected and successfully returned to the Earth in the Hayabusa2 mission. Fourier Transform Infrared Spectroscopy (FTIR) has been conducted to characterize these returned samples as one of the initial descriptions in a non-destructive manner under a purified nitrogen condition without terrestrial contamination. We selected the individual grains and aggregate samples that were not severely influenced by the reflection of incident beam at the sapphire dish and analyzed their reflectance spectra using the primary component analysis (PCA). The result indicates that Ryugu returned samples are highly homogeneous with only a little heterogeneity. The average spectrum of the main PCA group is represented by four absorption bands at 2.7, 3.05, 3.4, and 3.95 μm . The spectral feature is consistent with that obtained from bulk FTIR measurements, indicating potential presence of hydroxyl, organics, and carbonates. Rarely observed types of grains with unique spectra are categorized into three groups: significantly high reflectance, carbonates, and hydroxyl compounds with broad OH absorption.

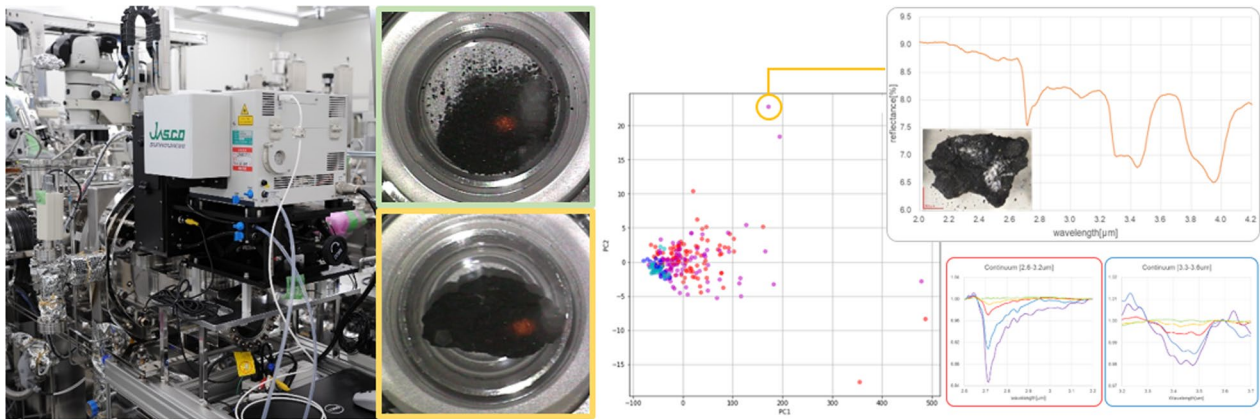
Keywords Hayabusa2, Ryugu returned samples, FTIR, Initial description, Curation

*Correspondence:

Kentaro Hatakeda
hatakeda@mwj.co.jp

Full list of author information is available at the end of the article

Graphical Abstract



Main text

Introduction

The Hayabusa2 spacecraft collected a total of ~5.4 g of sample at the surface of the C-type asteroid 162,173 Ryugu and successfully returned to the Earth in the mission (e.g., Tsuda et al. 2020; Tachibana et al. 2022). The collected samples were transported to the curation facility in the Institute of Space and Astronautical Science (ISAS), Japan Aerospace Exploration Agency (JAXA), in Sagami-hara, Japan, and stored in the clean chambers with purified nitrogen, except for a few grains picked up under vacuum condition, to keep these samples as physically and chemically pristine as possible. The uppermost centimeter-scale layer of Ryugu collected during the first touch-down sampling (TD1) was stored into the Chamber A of the sample catcher, while the surface to subsurface layer (a few meters) of Ryugu collected close to the artificial crater excavated by the impact of the small carry-on impactor (Arakawa et al. 2020) during the second touch-down sampling (TD2) was stored into the Chamber C. They were separately transferred to the “bulk” dishes (23 mm in diameter) made of sapphire glass placed in a stainless steel container (Yada et al. 2022). Then, initial descriptions for these returned samples have been performed, such as weighing, optical imaging, FTIR in 1–5 μm wavelength range (Yada et al. 2022), MicrOmega as a hyperspectral NIR microscope in 0.99–3.65 μm range (Pilorget et al. 2022), and visible multispectral imaging (Cho et al. 2022). Individual grains with the diameter larger than 1 mm and the aggregate samples consisting of sub-millimeter fine grains have been transferred from bulk dishes of Chambers A and C to small-sized sample dishes (15 and 10 mm in diameter) to be allocated for science community and also to

be archived for future research works. Initial descriptions for these samples were performed in the same manner as for the bulk samples.

Based on the NIR-FTIR and MicrOmega analysis on the bulk samples, returned Ryugu samples are represented by a deep OH absorption centered at 2.7 μm which is comparable to meter-scale remote sensing data by Near-Infrared Spectrometer (NIRS3) on board Hayabusa2 (Kitazato et al. 2019), and also by absorption between 3.3 and 3.5 μm centered at around 3.4 μm which is likely a series of overlapping vibrational features (Pilorget et al. 2022; Yada et al. 2022). MicrOmega spectral reflectance data also indicate sub-mm-scale features, such as carbonates with 2.3, 2.5, and large 3.3–3.5 μm absorptions and hydroxyl compounds with broad 3 μm absorption (Pilorget et al. 2022). Here we examined the homogeneity and heterogeneity of returned Ryugu samples with respect to the millimeter-scale NIR-FTIR spectra using the individual grains and aggregate samples.

Methods

System overview

The FTIR measurement system in this study consists of the spectrometer (VIR-300, JASCO Corporation) and the sample chamber (Fig. 1). The spectrometer is equipped with a Si/CaF₂ beam splitter and a liquid nitrogen-cooled indium antimonide (InSb) detector working in 1 to 5 μm spectral range. The standard light generated from a Halogen lamp passes through the sapphire glass viewport and illuminates the sample in the sample chamber with incidence and emission angles of 16°, and then reflects on the surface of the sample. A spot size of the incident light beam on the sample is approx. 1 mm diameter when the smallest aperture is used. The sample chamber

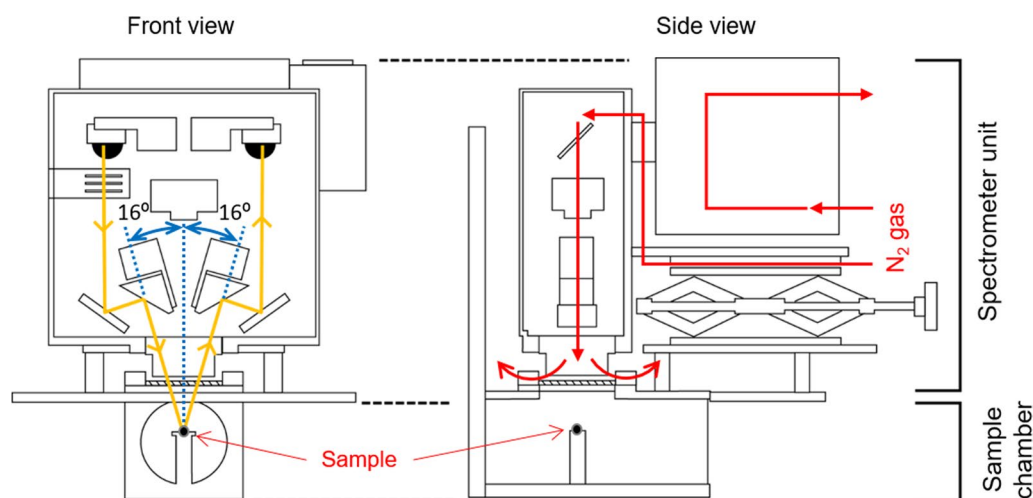


Fig. 1 Overview of the FTIR measurement system with front and side views of the spectrometer unit and the sample chamber. Yellow and red lines are the light path of the incident beam and nitrogen gas flow, respectively

is connected to the clean chamber and kept in purified nitrogen condition so that these samples are measured without atmospheric and particulate contamination. Since the spectrometer is not enclosed in the nitrogen condition, purified nitrogen is installed by flowing in the unit to reduce the influence of the absorptions caused in the atmosphere.

Measurement procedure

Background signal is obtained using the diffuse gold reflectance standard (Infragold, manufactured by Labsphere) placed inside the sample chamber to assume its reflectance value as 100%. Immediately after the background measurement, the gold standard (Infragold) was measured relative to itself (acting as sample and background), which should result in a spectrum having reflectance value of 100% at all wavelengths. Then it is noted that by doing this same measurement later (e.g., after Ryugu samples) it can be determined how the atmospheric conditions have evolved/changed during the course of the sample measurements. There are five absorption bands at 1.4, 1.85, 2.6–2.8, 3.1, and 4.2 μm in the background spectra (Fig. 2a). The absorption bands at 1.4, 1.85, 2.6–2.8 μm are derived from H_2O and that at 4.2 μm from CO_2 in atmosphere. The absorption band at 3.1 μm is possibly due to an instrumental artifact because in some cases the influence of H_2O and CO_2 appear as positive excursion in the Infragold measurement after sample analysis, but the 3.1 μm feature always appears as negative excursion. The other possibility is that the 3.1 μm feature comes from water–ice deposited in the InSb detector which is sometimes a problem with a nitrogen-cooled detector. The depths of these absorption

bands are less than 1% in most cases. The OH absorptions are basically not observed in the sample spectra, but shallow absorption at 2.6 μm might be due to the water in atmosphere (Fig. 2b and 2c). On the other hand, CO_2 absorption often appears in the sample spectra, which might be because the signal intensity rapidly decreases above 4.0 μm and the spectrum in that wavelength range is easily affected by the environmental change inside the spectrometer between the background and sample measurements, especially in low reflectance materials as the Ryugu samples (<5%). We concluded that atmospheric OH absorptions in the sample spectra are negligible level. On the other hand, atmospheric CO_2 absorption tends to influence on the sample spectra, and therefore, the spectral data at around 4.2 μm are not used in the analysis.

Samples used in this study are individual grains and aggregate samples which FTIR measurements were conducted before November 2021.

Effect of reflectance from sapphire dish

When the individual grain size is smaller than the beam spot size, the incident light beam partly reflects on the surface of a sample dish made of sapphire glass, which affects the reflectance spectrum of samples (Fig. 3). To evaluate the effect of reflected light from a sapphire dish, we measured different areas in the aggregate sample (A9009) where grains and particles are densely to sparsely distributed (positions 1–4) and the sapphire dish itself (position 5) as shown in Fig. 4. The reflectance of position 5 far exceeds 100% because the specular reflection from a sapphire dish is higher than the diffuse reflection from the Infragold. This examination is based on the

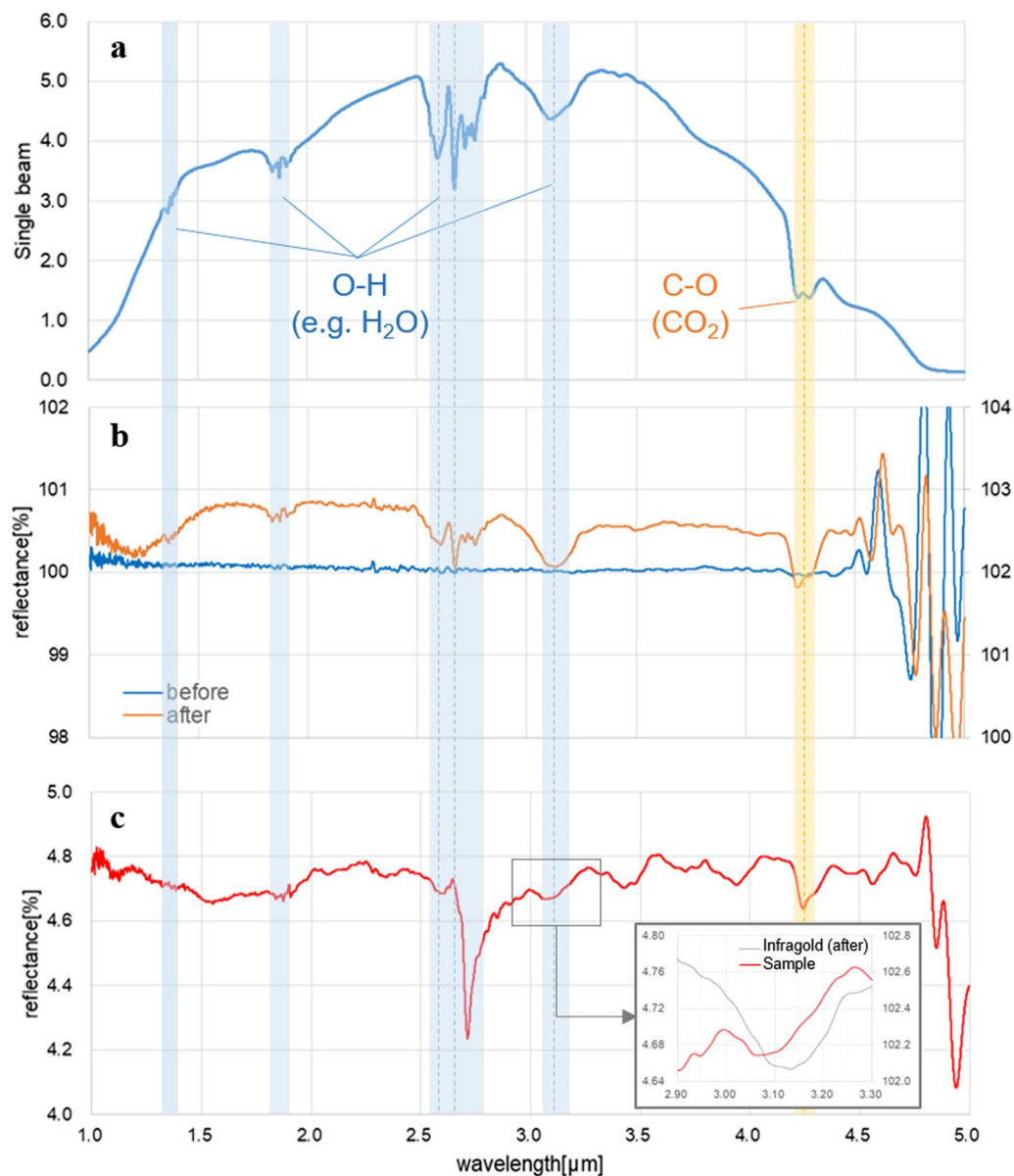


Fig. 2 Influence of absorption in atmosphere. Absorption bands of OH (1.4, 1.85, 2.6–2.8, 3.1 μm) and of CO₂ (4.2 μm) are detected in **a** background signal, and **b** Infragold spectra after the sample measurement (example of A0014). Basically no absorption band is detected in the Infragold spectra before the sample measurement. **c** Only CO₂ absorption is detected in the sample spectrum (example of A0014)

assumption that most of Ryugu grains and particles are spectrally homogeneous as described in the next chapter.

In terms of how the amount of sapphire material within the beam spot changes, with the increasing reflectance from a sapphire dish, the reflectance increases in entire wavelength range, the spectral slope changes from positive to negative especially in the wavelength of 1.0–2.5 μm, and the absorption band depth decreases (Fig. 4). Based on the result of this examination, we determined the samples significantly affected by the reflected light

from the sapphire dish which has negative spectral slope in entire wavelength range with less than 5% of shallow 2.7 μm absorption band. We excluded those samples and remaining 118 out of 205 individual grains and 9 out of 13 aggregate samples were used for data analysis.

Results and discussion

Principal component analysis (PCA)

We used the FTIR spectra of the samples in the range of 2.65–4.1 μm instead of the measurable wavelength range

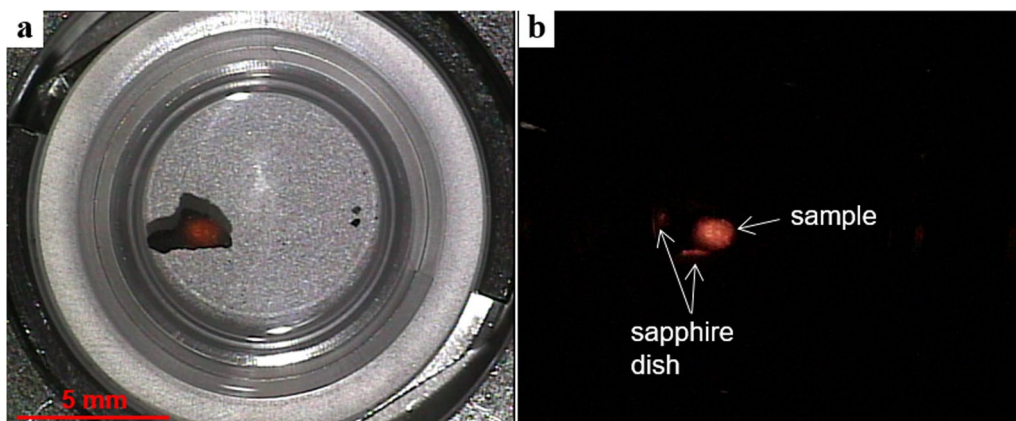


Fig. 3 Incident beam spot illuminating on the individual sample (C0033) and sapphire dish. Optical images with **a** internal light and **b** incident beam alone

of 1–5 μm , because a severe effect of reflectance from a sapphire dish mainly appears in the range of 1–2.5 μm , the absorption of atmospheric CO_2 often appears at 4.2 μm , and noisy spectra due to low signal intensity at 4.2–5 μm . PCA is a straightforward technique to be used for examination of spectral features by reducing the pertinent information in the spectra to a small number of components and PCA results can also be used to divide the data in groups (e.g., Bus and Binzel 2002; Paton et al. 2011). Total of 245 spectral data (197 for 118 individual grains and 48 for 9 aggregate samples) were analyzed using PCA (Additional file 1) and result is plotted in principal component space shown in Fig. 5. The PCA result indicates that the returned Ryugu samples are highly homogeneous (97% of individual grains are included in a single group) and only few samples show unique spectra.

Principal component 1 (PC1) is related to reflectance values of samples ($R^2 > 0.99$) represented by those at 2.65 μm where there is no absorption band in the selected wavelength range. Principal component 2 (PC2) seems to be related to the spectral slope between 2.65 and 4.1 μm ($R^2 = 0.82$) as shown in Fig. 6. Contribution rates of PC1 accounts for more than 99.7% and PC2 for 0.2% (Table 1). This indicates that the spectral variations of Ryugu samples are mostly explained by their reflectance variations, especially of individual grains which is much larger than those of aggregate samples (Fig. 5a). The large reflectance variation in the individual grains would be resulted from the effect of reflectance from a sapphire dish because the effect is observed in wavelength range of 1.0 to 2.5 μm in many of the individual grains.

Averaged reflectance spectrum of main group

Reflectance spectra of main groups including both individual grains and aggregate samples were normalized to

2.65–4.1 μm continuum and averaged to examine the spectral features. Reflectance of each spectrum was first normalized at the wavelength of 2.0 μm . Then, a straight line continuum was made to fit in wavelength between 2.65 and 4.1 μm , and the spectrum was modified as flat continuum between 2.65 and 4.1 μm (Fig. 7).

The averaged spectrum of main group is represented by four absorption bands at 2.7, 3.05, 3.4, and 3.95 μm (Fig. 8), which is consistent with the FTIR spectra obtained from the bulk Ryugu samples (Yada et al. 2022). The prominent deep absorption centered at 2.72 μm is one of the typical characteristics of Ryugu indicating the presence of hydroxyl, detected not only by FTIR but also by MicrOmega (Pilorget et al. 2022) and by NIRS3 remote sensing (Kitazato et al. 2019). Absorption bands at 3.05 and 3.4 μm are indicated as possible organic materials. Pilorget et al. (2022) interpreted that the 3.05 and 3.4 μm bands indicate the N–H-rich and C–H-rich compounds, respectively, but carbonate absorption is also present at 3.4 μm . The absorption band at 3.95 μm is only detected by FTIR because the spectral range of MicrOmega is up to 3.64 μm . The fact that this absorption band always appears with that at 3.4 μm in the samples analyzed in this study, the 3.95 μm absorption band coexisting with 3.4 μm band would indicate the presence of carbonate. Supportively Fig. 9 shows the deformation of carbonate spectral feature by shifting the measurement area. This is probably because the carbonate-rich area in the incident beam spot was reduced by shifting the measurement area.

Averaged reflectance spectrum of individual grains (2.65–4.1 μm) and aggregate samples included in the main group of PCA plot show similar spectral profiles to that of bulk samples analyzed in Yada et al. (2022) in terms of the presence of absorption bands at 2.7,

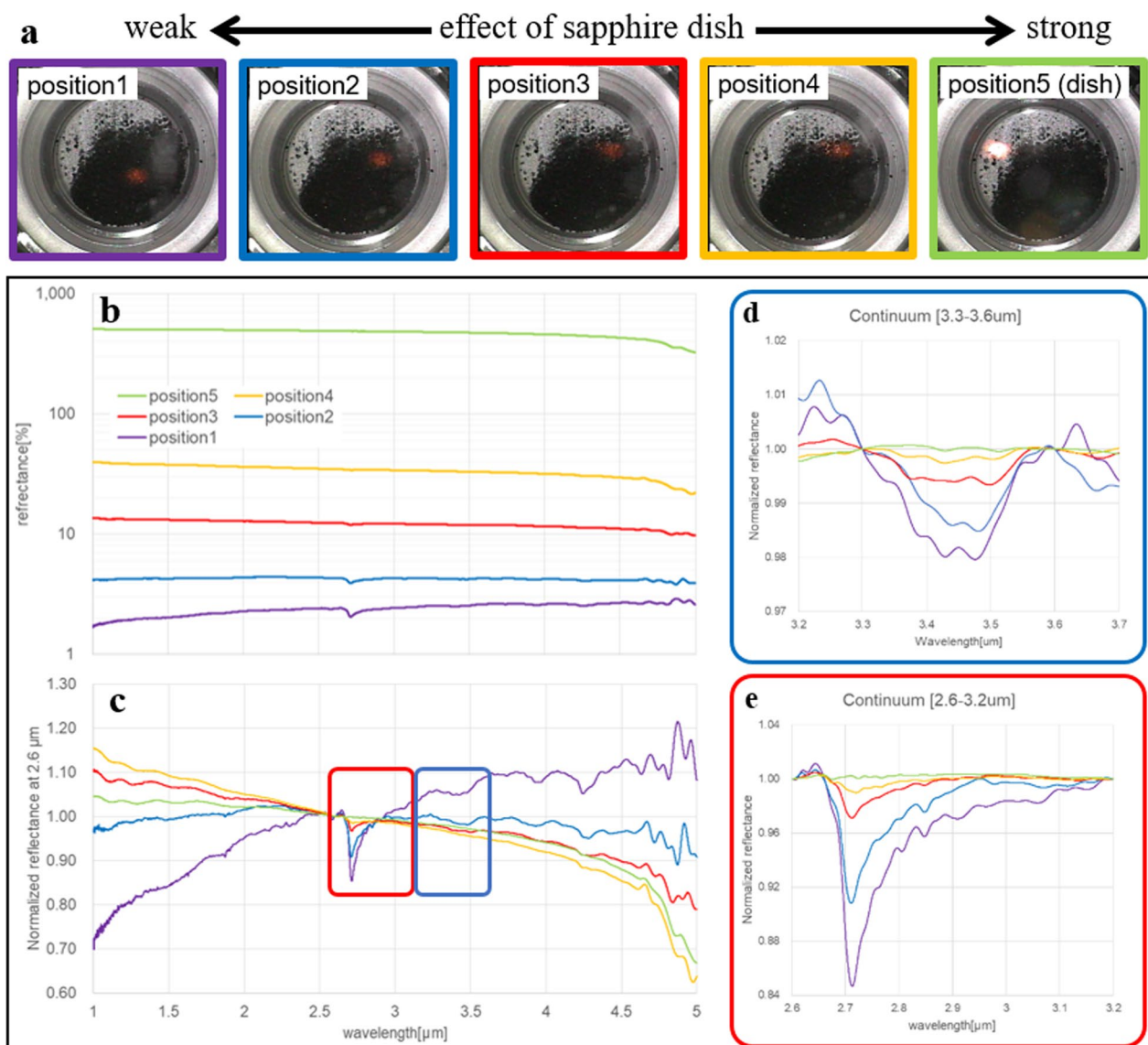


Fig. 4 Effect of reflectance from sapphire dish. **a** Measurement areas on the aggregate sample, A9009. Grains and particles are fully occupied in the beam spot in position 1. Measurement spots were then shifted to the edge of the aggregate sample and void ratio increases from position 2 to 4. Sapphire dish itself is measured in position 5. **b** Reflectance spectra of each measurement area increasing from positions 1 to 5. **c** Reflectance spectra normalized at 2.6 μm to compare the spectral profiles of positions 1 to 5. **d** Normalized reflectance spectra continuum with 2.6–3.2 μm, and **e** 3.3–3.6 μm show the change in absorption band depth from positions 1 to 5

3.05, 3.4, and 3.95 μm, and spectral slope is also similar between the aggregate and bulk samples (Fig. 10a). On the other hand, individual grains and aggregate samples are higher in reflectance and larger in variation of absorption band depth at 2.7 μm compared to those of bulk samples (Fig. 10b, c). Higher reflectance and large variation of 2.7 μm band depth of individual grains are mainly explained by the effect of reflectance from a sapphire dish which is observed in the wavelength range of 1.0 to 2.5 μm in many of the samples. The difference

between aggregate and bulk samples would be caused by the difference of incident beam spot size which is approx. 1 mm for the aggregate samples (as well as the individual grains) and approx. 6 mm for the bulk samples. The smaller beam spot would be more sensitive to the influence of surface morphology, especially of the locally high reflectance area. The spectral profile of the aggregate sample is also comparable with the averaged bulk sample spectra by MicrOmega (Pilorget et al. 2022).

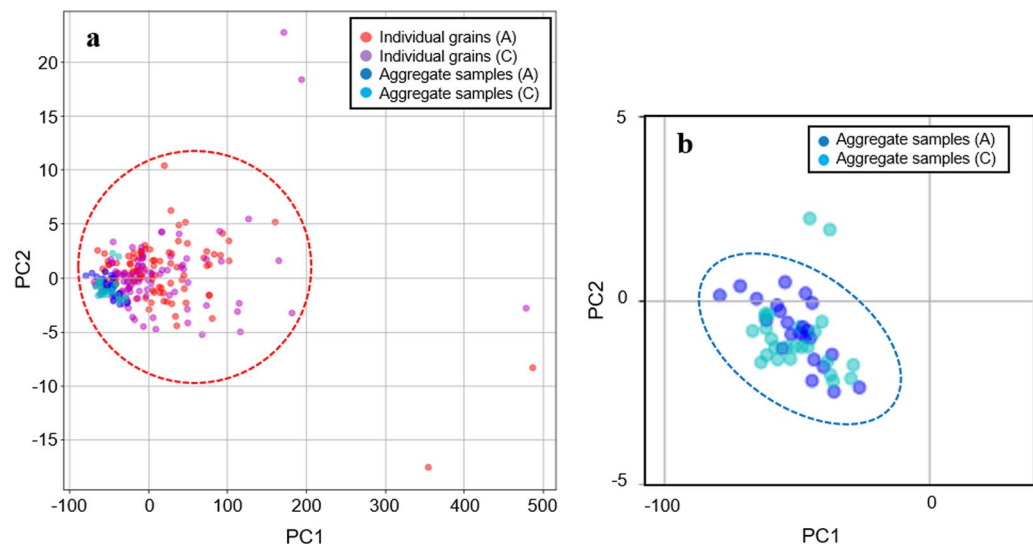


Fig. 5 PCA plot for **a** all the reflectance spectra including individual grains and aggregate samples, and for **b** spectra for aggregate samples. Spectra inside the dashed line are included as the homogeneous group. No difference is observed between the samples from chambers A and C

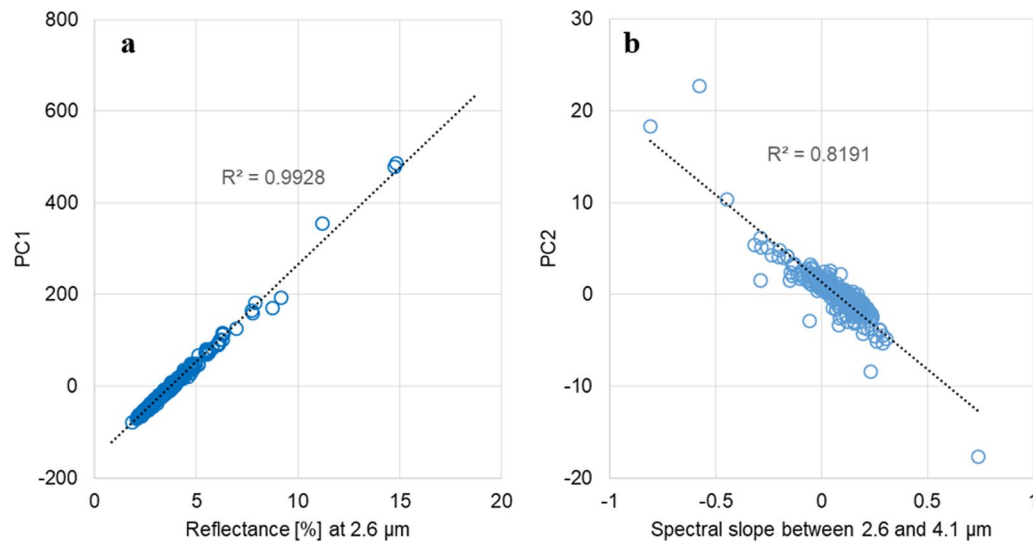


Fig. 6 Parameters related to PC1 and PC2. **a** PC1 is highly correlative with the reflectance of samples represented at 2.6 μm. **b** PC2 seems to correlate with the spectral slope in the analyzed wavelength range (2.6–4.1 μm)

Table 1 Contribution rate of PCA (PC1 to PC5) for individual grains and aggregate samples

	Contribution rate
PC1	0.9976073
PC2	0.0018695
PC3	0.0002893
PC4	0.0000875
PC5	0.0000439

PC1 accounts for more than 99.7% of contribution rate

Detailed mineralogical analysis using a part of Ryugu samples (e.g., Ito et al. 2022, Nakamura et al. 2022a, b) reported that the Ryugu grains mainly consist of phyllo-silicate-rich (saponite and serpentine) matrix with fine grained (10's of μm to sub-micrometer) components, such as carbonates, Fe sulfides, phosphates, magnetite, olivine, and pyroxene. Carbonate minerals are commonly observed in the Ryugu grains, in which fine grained dolomite is the most abundant and breunnerite is less abundant but occurs as larger crystals (Nakamura et al. 2022a;

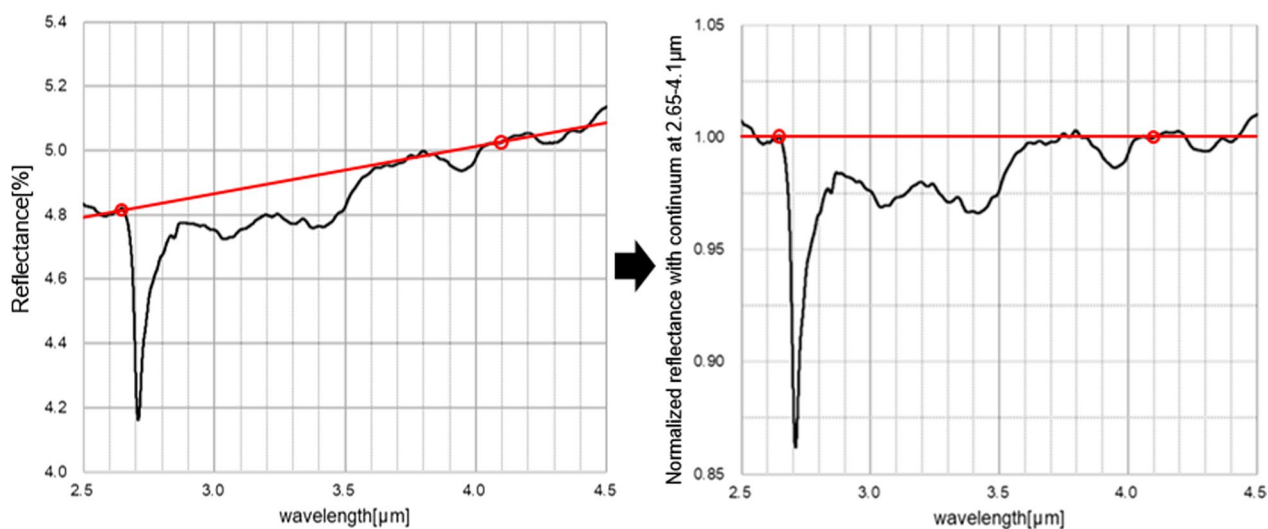


Fig. 7 Procedure to make reflectance spectrum with normalized to 2.65–4.1 μm continuum

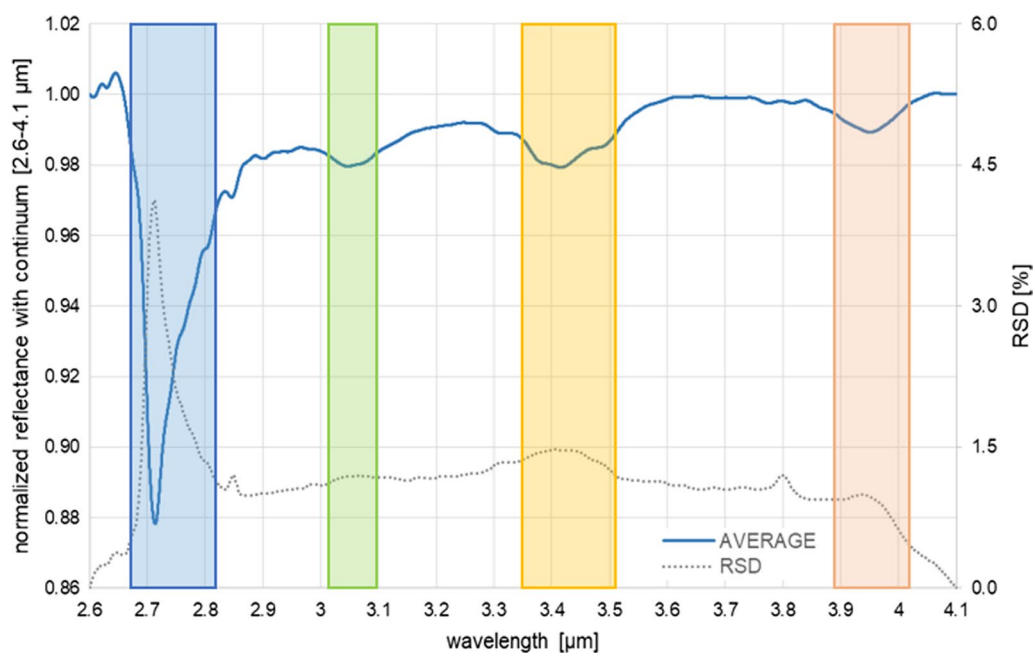


Fig. 8 Averaged spectrum of individual grains included in main group in the PCA plot. Relative standard deviation is also plotted with the dashed line. The spectrum is represented by absorption bands at 2.7 μm (blue), 3.05 μm (green), 3.4 μm (orange), and 3.95 μm (red)

b). The carbonate feature as observed in averaged spectra of individual grains, aggregate, and bulk samples in this study would reflect the common occurrence of carbonates in the Ryugu returned samples, mainly derived from fine grained dolomite. On the other hand, distinct carbonate spectral feature observed in A0059 in Fig. 9, and C0041 (as shown below) might be derived from large breunnerite grains.

Heterogeneity in the returned Ryugu samples

As the result of PCA, returned Ryugu samples rarely contain the grains with unique spectra detected by NIR-FTIR analysis. In this study, we obtained three types of unique spectral features; carbonates with two deep broad absorptions at 3.3–3.5 and 3.8–4.0 μm (Figs. 11a, 12b), the ones represented by significantly high reflectance (approx. 15%, Fig. 11b–d), and hydroxyl (–OH-rich)

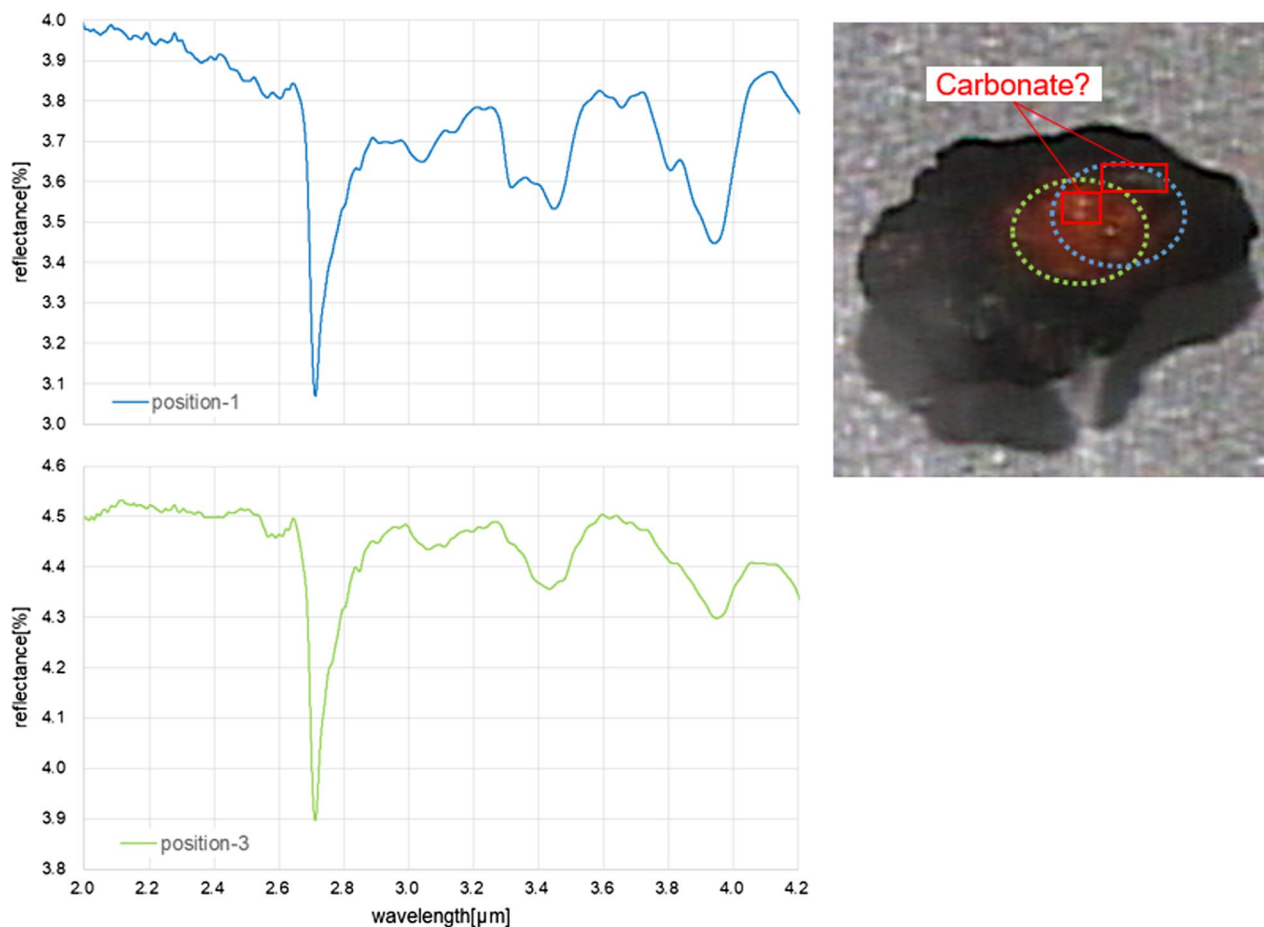


Fig. 9 Deformation of carbonate spectral feature by shifting the measurement area observed in A0059. Dashed circles on the optical images show measurement areas corresponding to the spectra of position 1 (blue) and position 3 (green). Carbonate inclusion is not apparently visible but might be the small white areas on the grain

compounds indicating broad absorption between 2.65 and 4.0 μm with maximum absorption at around 2.7 μm (Fig. 12a). The significantly high reflectance samples accounts for 2.5% (3 out of 118 samples) and the sample including large carbonate for 0.8% (1 of 118) of the individual grains. On the other hand, Nakato et al. (2023) represented that grains with white components with more than $>300\mu\text{m}^2$ accounted for 6% of 205 individual grains based on the optical microscopic images. They are considered as carbonates or compounds with broad OH absorption, but most of them are much smaller than the spot size (approx. 1 mm in diameter) of the FTIR and their spectral characteristics would be hidden by the surrounding matrix spectra. The grains with broad OH absorption are always found as sub-mm-sized grain and not observed in the individual grains of larger than 1 mm in size. Carbonates and compounds with broad OH absorption were also detected by MicrOmega as sub-mm grains or clasts/inclusions in the bulk samples (Pilorget et al. 2022). Extraordinary high reflectance in samples

A0038 and C0079 contain flat metallic face on their surface. On the other hand, high reflectance of A0054 without apparent clast/inclusion might be explained by specular reflection by flat smooth surface facing upwards on the grain (Yumoto et al. 2022). Based on the optical microscopic images, the metallic components in A0038 and C0079 seem to be aggregates of very fine bright particles surrounded by relatively rough and coarse grained dark matrix. Similar structure was found in the polished section of A0035 by Nakamura et al. (2022a). The structure called “massive domain” is light-colored region of several 100’s μm in size containing abundant fine grained (<10 ’s of μm) Fe sulfide distinct from the surrounding matrix predominantly composed of phyllosilicate with coarse grained (10’s of μm to 100 μm) components, such as carbonate, phosphate, Fe sulfide, magnetite, olivine, and pyroxene. This implies that the metallic phases rarely found in Ryugu grains are aggregates of fine grained (<10 ’s of μm) components with abundant Fe sulfides.

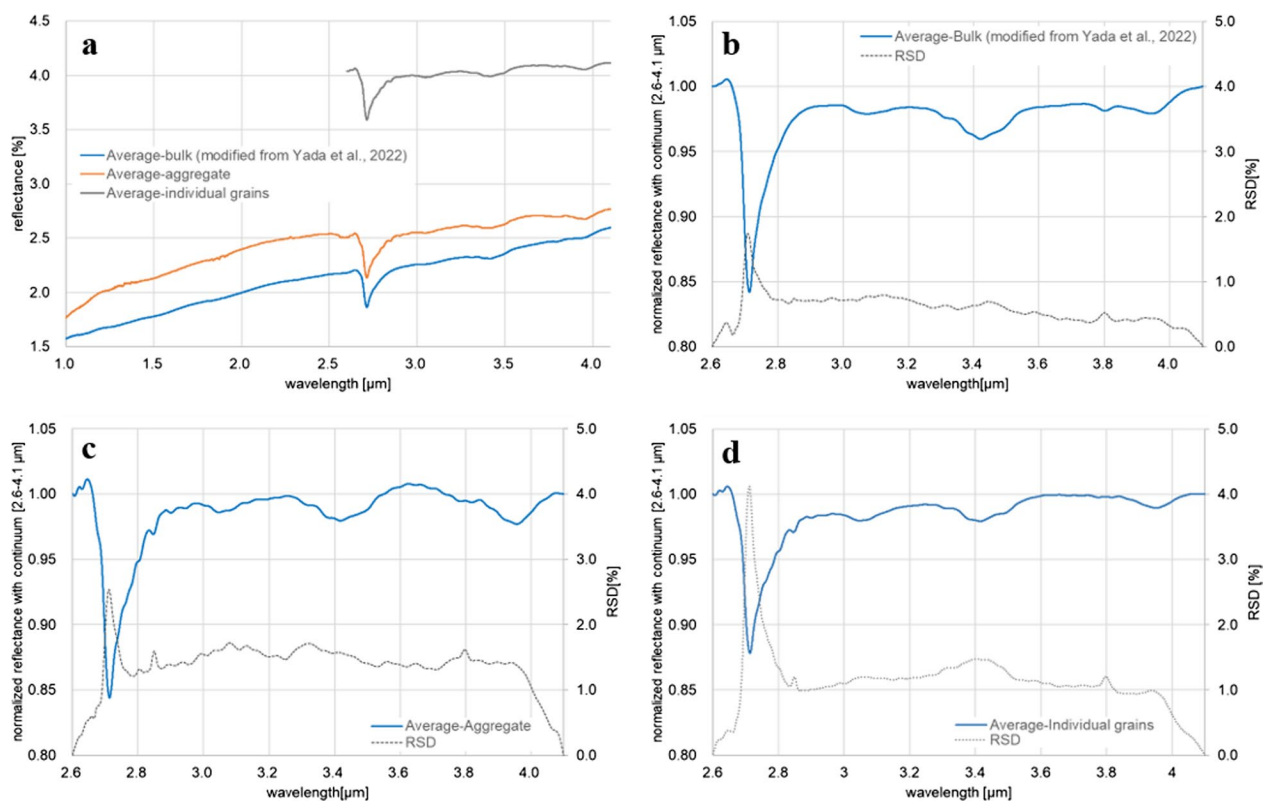


Fig. 10 Comparison of averaged reflectance spectra among the bulk samples, aggregate samples, and individual grains. Averaged **a** absolute reflectance and normalized reflectance with continuum at 2.6–4.1 μm for **b** bulk samples, **c** aggregate samples, and **d** individual grains. Beam spot size of bulk samples is approx. 6 mm, and that of aggregate samples and individual grains is approx. 1 mm. Relative standard deviation (RSD, %) is also shown in **b**, **c**, and **d**

In conclusion, FTIR spectroscopy under the purified nitrogen condition is a powerful tool to estimate minerals and chemical components in extraterrestrial materials recovered by sample return missions without any of terrestrial contamination and with non-destructive manner, including the damage on samples by heat, UV, and X-rays. In this study, hydroxyls in phyllosilicates and carbonates are detected in the Ryugu returned samples with the wavelength range of 1–5 μm. More detailed characterization of samples by improving the FTIR system for the future sample return missions, such as OSIRIS-REx and MMX, will be significantly valuable for researchers to select samples suitable for their investigations. It is expected to detect a variety of organics features and mineral components by extending the measurable wavelength range to Mid-infrared and also to identify the specific sub-mm-sized spectral features within a single grain by narrowing the beam spot.

Summary

Near-infrared FTIR spectrometric analysis has been conducted for individual grains and aggregate samples transferred from bulk Ryugu samples. We evaluated

the effect of reflectance from the sample dishes made from sapphire and revealed that with increasing the sapphire effect, reflectance in entire wavelength range increases, the spectral slope especially in 1.0–2.5 μm changes from positive to negative, and the absorption band depth decreases. Total of 245 spectral data in 118 samples without or less affected by the sapphire sample dish were processed using PCA, and the result indicates high homogeneity of Ryugu samples. Averaged spectrum of main (homogeneous) group is represented by four absorption bands at 2.7, 3.05, 3.4, and 3.95 μm which are consistent with those of bulk samples analysis by FTIR. The 3.95 μm absorption band is only detected by FTIR, and coexistence of 3.4 and 3.95 μm bands implies the presence of carbonate. Comparison of average spectra and variability in absorption band depth at 2.7 μm between individual grains, aggregate, and bulk samples indicates that significantly high reflectance and large variation of band depth in individual grains than the others would be caused by the effect of reflectance from sapphire dishes, and slightly higher reflectance and variation of band depth in aggregate samples than in the bulk samples are possibly due to the smaller spot size in aggregate

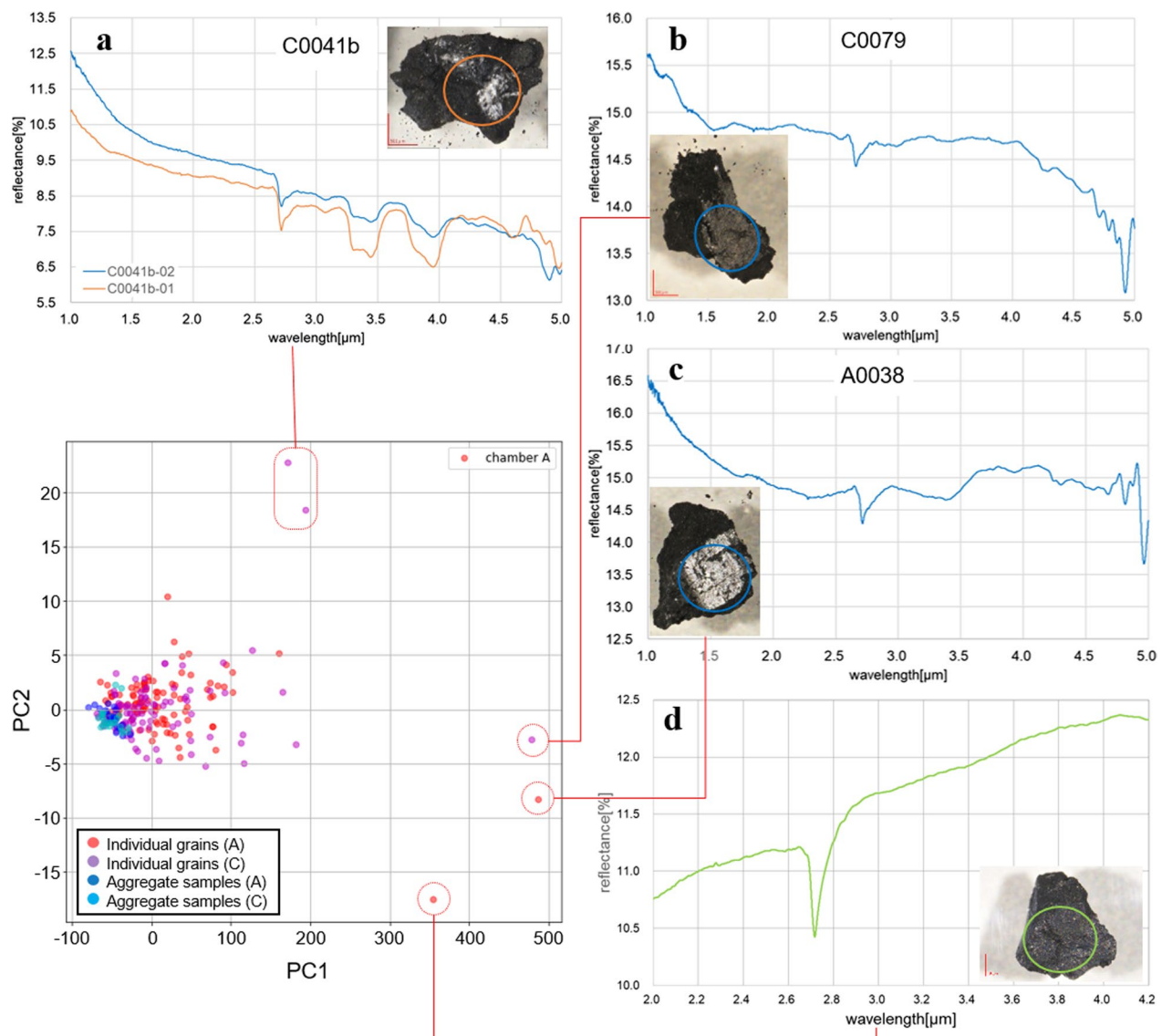


Fig. 11 Rarely detected unique spectra in individual grains: **a** C0041b, large carbonate inclusion, **b, c** C0079 and A0038, high reflectance with metallic inclusion, **d** C0054, high reflectance with specular reflection. The enclosed areas in the optical microscope images indicate the beam spots

samples which would be more sensitive to the sample surface morphology. Samples with unique spectral features are rarely found, and there are three types: the one with significantly high reflectance, carbonate with two deep broad absorptions at 3.3–3.5 and 3.8–4.0 μm , and hydroxyl compound with broad OH absorption peaked at around 2.7 μm . The grains with high reflectance spectra contain flat and metallic clasts/inclusions which are

considered to be an aggregate of fine grained components dominated by Fe sulfides. Carbonate features as observed in averaged spectra of individual grains, aggregate, and bulk samples possibly indicate the common occurrence of carbonate minerals mainly derived from fine grained dolomite in Ryugu grains/particles, while distinct carbonate features observed in specific samples would be derived from large clasts/inclusions of breunnerite.

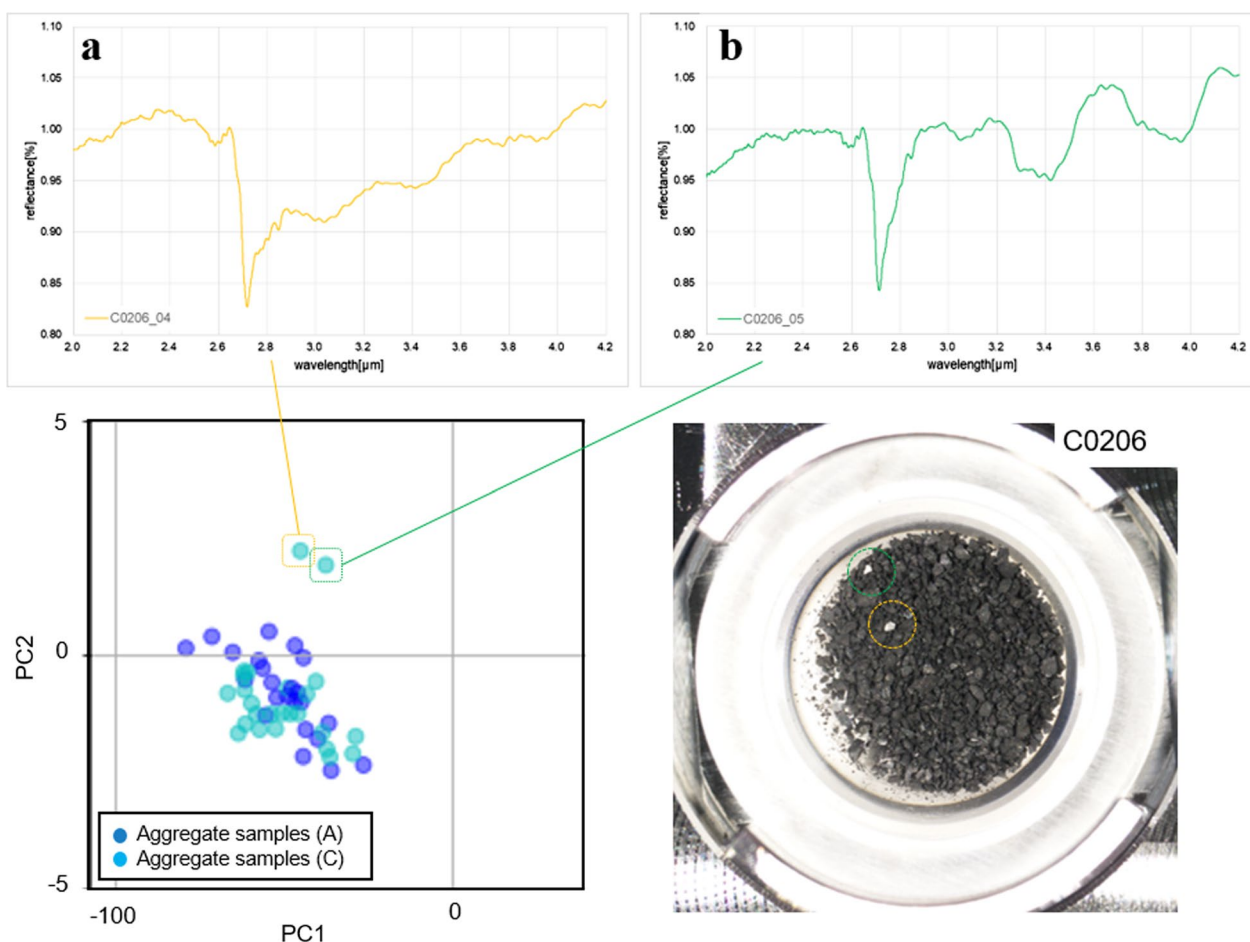


Fig. 12 Rarely detected unique spectra in aggregate samples: **a** carbonate in aggregate sample, C0206, **b** hydroxyl component with broad OH absorption in aggregate sample, C0206. The enclosed areas in the optical microscope images indicate the beam spots

Abbreviations

C-type	Carbonaceous-type
ISAS	Institute of Space and Astronautical Science
JAXA	Japan Aerospace Exploration Agency
TD	Touch-Down
NIR	Near-Infrared
FTIR	Fourier Transform InfraRed
NIRS3	Near-Infrared Spectrometer
PCA	Principal Component Analysis

Supplementary Information

The online version contains supplementary material available at <https://doi.org/10.1186/s40623-023-01784-w>.

Additional file 1. Samples and number of spots used for PCA.

Acknowledgements

The authors are sincerely grateful to Hayabusa2 project team for development and operations of the Hayabusa2 spacecraft throughout the sample return mission. They thank Hayabusa2 Sampler team for transportation of sample capsule to ISAS/JAXA and installing the sample container to the clean chamber in the Extraterrestrial Sample Curation Center (ESCuC) of JAXA. They thank Dr. Kentaro Uesugi (SPRING-8/JASRI) for designing and developing the sample holders and some of the sample handling tools, and also Dr. Yuji Yamamoto

(Kochi University) and Dr. Motoo Ito (JAMSTEC/KCC) for developing the procedure of demagnetizing sample handling tools. Dr. Rosario Brunetto, a handling editor, and two anonymous reviewers gave us the helpful comments.

Author contributions

KH conducted sample processing and data acquisition with TY, AN, KY, AM, KKu, and YH and summarized the data for manuscript preparation. MH, HS, and KN contributed to data management. AI, MY, and SF contributed to instrumental and environmental preparation for sample analysis. MA, TO, TU, and KKi supervised the research. All the authors read and approved the final manuscript.

Funding

Not applicable.

Availability of data and materials

All the initial description data for Ryugu returned samples are available in the database titled "Hayabusa2, Ryugu Sample Curatorial Dataset" (<https://doi.org/10.17597/ISAS.DARTS/CUR-Ryugu-description>). The database publications are compliant with ISAS data policies (<https://www.isas.jaxa.jp/en/researchers/data-policy/>).

Declarations

Ethics approval and consent to participate

Not applicable.

Consent for publication

Not applicable.

Competing interests

The authors declare that they have no competing interests.

Author details

¹Institute of Space and Astronautical Science (ISAS), Japan Aerospace Exploration Agency (JAXA), Sagami-hara, Kanagawa 252-5210, Japan. ²Marine Works Japan Ltd, 3-54-1 Oppama-Higashi, Yokosuka 237-0063, Japan. ³The Graduate University for Advanced Studies (SOKENDAI), Hayama 240-0193, Japan. ⁴University of Tokyo, Bunkyo City, Tokyo 113-0033, Japan. ⁵The University of Aizu, Aizu-Wakamatsu 965-8580, Japan.

Received: 20 August 2022 Accepted: 10 February 2023

Published online: 28 March 2023

References

- Arakawa M, Saiki T, Wada K, Ogawa K, Kadono T, Shirai K, Sawada H, Ishibashi K, Honda R, Sakatani N, Iijima Y, Okamoto C, Yano H, Takagi Y, Hayakawa M, Michel P, Jutzi M, Shimaki Y, Kimura S, Mimasu Y, Toda T, Imamura H, Nakazawa S, Hayakawa H, Sugita S, Morota T, Kameda S, Tatsumi E, Cho Y, Yoshioka K, Yokota Y, Matsuoka M, Yamada M, Kouyama T, Honda C, Tsuda Y, Watanabe S, Yoshikawa M, Tanaka S, Terui F, Kikuchi S, Yamaguchi T, Ogawa N, Ono G, Yoshikawa K, Takahashi T, Takei Y, Fujii A, Takeuchi H, Yamamoto Y, Okada T, Hirose C, Hosoda S, Mori O, Shimada T, Soldini S, Tsukizaki R, Iwata T, Ozaki M, Abe M, Namiki N, Kitazato K, Tachibana S, Ikeda H, Hirata N, Hirata N, Noguchi R, Miura A (2020) An artificial impact on the asteroid (162173) Ryugu formed a crater in the gravity-dominated regime. *Science* 368:67–71. <https://doi.org/10.1126/science.aaz1701>
- Bus SJ, Binzel RP (2002) Phase II of the small main-belt asteroid spectroscopic survey: the observations. *Icarus* 158:106–145. <https://doi.org/10.1006/icar.2002.6857>
- Cho Y, Yumoto K, Yabe Y, Mori S, Ogura JA, Yada T, Miyazaki A, Yogata K, Hatakeda K, Nishimura M, Abe M, Usui T, Sugita S (2022) Development of a multispectral stereo-camera system comparable to Hayabusa2 Optical Navigation Camera (ONC-T) for observing samples returned from asteroid (162173) Ryugu. *Planet Space Sci* (in Press). <https://doi.org/10.1016/j.pss.2022.105549>
- Ito M, Tomioka N, Uesugi M, Yamaguchi A, Shirai N, Ohigashi T, Liu MC, Greenwood RC, Kimura M, Imae N, Uesugi K, Nakato A, Yogata K, Yuzawa H, Kodama Y, Tsuchiyama A, Yasutake M, Findlay R, Franchi IA, Malley JA, McCain KA, Matsuda N, McKeegan KD, Hirahara K, Takeuchi A, Sekimoto S, Sakurai I, Okada I, Karouji Y, Arakawa M, Fujii A, Fujimoto M, Hayakawa M, Hirata N, Hirata N, Honda R, Honda C, Hosoda S, Iijima Y, Ikeda H, Ishiguro M, Ishihara Y, Iwata T, Kawahara K, Kikuchi S, Kitazato K, Matsuoka M, Matsuoka M, Michikami T, Mimasu Y, Miura A, Mori O, Morota T, Nakazawa S, Namiki N, Noda H, Noguchi R, Ogawa N, Ogawa K, Okada T, Okamoto C, Ono G, Ozaki M, Saiki T, Sakatani N, Sawada H, Senshu H, Shimaki Y, Shirai K, Sugita S, Takei Y, Takeuchi H, Tanaka S, Tatsumi E, Terui F, Tsukizaki R, Wada K, Yamada M, Yamada T, Yamamoto Y, Yano H, Yokota Y, Yoshihara K, Yoshikawa M, Yoshikawa K, Fukai R, Furuya S, Hatakeda K, Hayashi T, Hitomi Y, Kumagai K, Miyazaki A, Nishimura M, Soejima H, Iwamae A, Yamamoto D, Yoshitake M, Yada T, Abe M, Usui T, Watanabe S, Tsuda Y (2022) A pristine record of outer solar system materials from asteroid Ryugu's returned sample. *Nat Astron*. <https://doi.org/10.1038/s41550-022-01745-5>
- Kitazato K, Milliken RE, Iwata T, Abe M, Ohtake M, Matsuura S, Arai T, Nakauchi Y, Nakamura T, Matsuoka M, Senshu H, Hirata N, Hiroi T, Pilorget C, Brunetto R, Poulet F, Riu L, Bibring J-P, Takir D, Domingue DL, Vilas F, Barucci MA, Perna D, Palomba E, Galiano A, Tsumura K, Osawa T, Komatsu M, Nakato A, Arai T, Takato N, Matsunaga T, Takagi Y, Matsumoto K, Kouyama T, Yokota Y, Tatsumi E, Sakatani N, Yamamoto Y, Okada T, Sugita S, Honda R, Morota T, Kameda S, Sawada H, Honda C, Yamada M, Suzuki H, Yoshioka K, Hayakawa M, Ogawa K, Cho Y, Shirai K, Shimaki Y, Hirata N, Yamaguchi A, Ogawa N, Terui F, Yamaguchi T, Takei Y, Saiki T, Nakazawa S, Tanaka S, Yoshikawa M, Watanabe S, Tsuda Y (2019) The surface composition of asteroid 162173 Ryugu from Hayabusa2 near-infrared spectroscopy. *Science* 364:272–275. <https://doi.org/10.1126/science.aav7432>
- Nakamura E, Kobayashi K, Tanaka R, Kunihiro T, Kitagawa H, Potisizil C, Ota T, Sakaguchi C, Yamanaka M, Ratnayake DM, Tripathi H, Kumar R, Avramescu M-L, Tsuchida H, Yachi Y, Miura H, Abe M, Fukai R, Furuya S, Hatakeda K, Hayashi T, Hitomi Y, Kumagai K, Miyazaki A, Nakato A, Nishimura M, Okada T, Soejima H, Sugita S, Suzuki A, Usui T, Yada T, Yamamoto D, Yogata K, Yoshitake M, Arakawa M, Fujii A, Hayakawa M, Hirata N, Hirata N, Honda R, Honda C, Hosoda S, Iijima Y, Ikeda H, Ishiguro M, Ishihara Y, Iwata T, Kawahara K, Kikuchi S, Kitazato K, Matsumoto K, Matsuoka M, Michikami T, Mimasu Y, Miura A, Morota T, Nakazawa S, Namiki N, Noda H, Noguchi R, Ogawa N, Ogawa K, Okamoto C, Ono G, Ozaki M, Saiki T, Sakatani N, Sawada H, Senshu H, Shimaki Y, Shirai K, Takei Y, Takeuchi H, Tanaka S, Tatsumi E, Terui F, Tsukizaki R, Wada K, Yamada M, Yamada T, Yamamoto Y, Yano H, Yokota Y, Yoshihara K, Yoshikawa M, Yoshikawa K, Fujimoto M, Watanabe S, Tsuda Y (2022a) On the origin and evolution of the asteroid Ryugu: a comprehensive geochemical perspective. *Proc Jpn Acad Ser B* 98:227–282. <https://doi.org/10.2183/pjab.98.015>
- Nakamura T, Matsumoto M, Amano K, Enokido Y, Zolensky ME, Mikouchi T, Genda H, Tanaka S, Zolotov MY, Kurosawa K, Wakita S, Hyoudo R, Nagano H, Nakashima D, Takahashi Y, Fujioka Y, Kikuri M, Kagawa E, Matsuoka M, Brealey AJ, Tsuchiyama A, Uesugi M, Matsumoto J, Kimura Y, Sato M, Milliken RE, Tatsumi E, Sugita S, Hiroi T, Kitazono K, Brownlee D, Joswiak DJ, Takahashi M, Ninomiya K, Osawa T, Terada K, Brenker FE, Tkalcic BJ, Vincze L, Brunetto R, Aleon-Toppiani A, Chan QHS, Roskosz M, Vinnet J-C, Beck P, Alp EE, Michikami T, Nagaishi Y, Tsuji T, Ino Y, Martinez J, Han J, Dolocan A, Bodnar RJ, Tanaka M, Yoshida H, Sugiyama K, King AJ, Fukushi K, Suga H, Yamashita S, Kawai T, Inoue K, Nakato A, Noguchi T, Vilas F, Hendrix AR, Jaramillo-Correa C, Domingue DL, Dominguez G, Gainsforth Z, Engrand C, Duprat J, Russell SS, Bonato E, Ma C, Kawamoto T, Wada T, Watanabe S, Endo R, Enju S, Riu L, Rubino S, Tack P, Takeshita S, Takeichi Y, Takeuchi A, Takigawa A, Takir D, Tanigaki T, Taniguchi A, Tsukamoto K, Yagi T, Yamada S, Yamamoto K, Yamashita Y, Yasutake M, Uesugi K, Umegaki I, Chiu I, Ishizaki T, Okumura S, Palomba E, Pilorget C, Potin SM, Alasli A, Anada S, Arai Y, Sakatani N, Schulz C, Sekizawa O, Sitzman SD, Sugiyama K, Sun M, Dartois E, De Pauw E, Dionnet Z, Djouadi Z, Falkenberg G, Fujita R, Fukuma T, Gearba IR, Hagita K, Hu MY, Kato T, Kawamura T, Kimura M, Kubo MK, Langenhorst F, Lantz C, Lavina B, Lindner M, Zhao J, Vekemans B, Baklouti D, Bazi B, Borondics F, Nagasawa S, Nishiyama G, Nitta K, Mathurin J, Matsumoto T, Mitsukawa I, Miura H, Miyake A, Miyake Y, Yurimoto H, Okazaki R, Yabuta H, Naraoka H, Sakamoto K, Tachibana S, Connolly HC Jr, Lauretta DS, Yoshitake M, Yoshikawa M, Yoshikawa K, Yoshihara K, Yokota Y, Yogata K, Yano H, Yamamoto Y, Yamamoto D, Yamamoto Y, Yamada T, Yada T, Wada K, Usui T, Tsukizaki R, Terui F, Takeuchi H, Takei Y, Iwamae A, Soejima H, Shirai K, Shimaki Y, Senshu H, Sawada H, Saiki T, Ozaki M, Ono G, Okada T, Ogawa N, Ogawa K, Noguchi R, Noda H, Nishimura M, Namiki N, Nakazawa S, Morota T, Miyazaki A, Miura A, Mimasu Y, Matsumoto K, Kumagai K, Kouyama T, Kikuchi S, Kawahara K, Kameda S, Iwata T, Ishihara Y, Ishiguro M, Ikeda H, Hosoda S, Honda R, Honda C, Hitomi Y, Hirata N, Hirata N, Hayashi T, Hayakawa M, Hatakeda K, Furuya S, Fukai R, Fujii A, Cho Y, Arakawa M, Abe M, Watanabe S, Tsuda Y (2022b) Formation and evolution of carbonaceous asteroid Ryugu: direct evidence from returned samples. *Science*. <https://doi.org/10.1126/science.abn8671>
- Nakato A, Yada T, Nishimura M, Yogata K, Miyazaki A, Nagashima K, Hatakeda K, Kumagai K, Hitomi Y, Soejima H, Bibring JP, Pilorget C, Hamm V, Brunetto R, Riu L, Lourit L, Loizeau D, Le Pivert-Jolivet T, Lequertier G, Moussi-Soffys A, Abe M, Okada T, Usui T, Nakazawa S, Saiki T, Tanaka S, Terui F, Yoshikawa M, Tsuda Y (2023) Variations of the surface characteristics of Ryugu returned samples. *Earth Planets Space*. <https://doi.org/10.1186/s40623-022-01754-8>
- Paton M, Muinonen K, Pesonen LJ, Kuosmanen V, Kohout T, Laitinen J, Lehtinen M (2011) A PCA study to determine how features in meteorite reflectance spectra vary with the samples' physical properties. *J Quant Spectrosc Radiat Transfer* 112:1803–1814. <https://doi.org/10.1016/j.jqsrt.2011.01.033>
- Pilorget C, Okada T, Hamm V, Brunetto R, Yada T, Loizeau D, Riu L, Usui T, Moussi-Soffys A, Hatakeda K, Nakato A, Yogata K, Abe M, Aleon-Toppiani A, Carter J, Chaigneau M, Crane B, Gondet B, Kumagai K, Langevin Y, Lantz C, Le Pivert-Jolivet T, Lequertier G, Lourit L, Miyazaki A, Nishimura M, Poulet F, Arakawa M, Hirata N, Kitazato K, Nakazawa S, Namiki N, Saiki T, Sugita S, Tachibana S, Tanaka S, Yoshikawa M, Tsuda Y, Watanabe S, Bibring JP (2022) First compositional analysis of Ryugu samples by the MicroOmega hyperspectral microscope. *Nat Astron* 6:221–225. <https://doi.org/10.1038/s41550-021-01549-z>

- Tachibana S, Sawada H, Okazaki R, Takano Y, Sakamoto K, Miura YN, Okamoto C, Yano H, Yamanouchi S, Michel P, Zhang Y, Schwartz S, Thuillet F, Yurimoto H, Nakamura T, Noguchi T, Yabuta H, Naraoka H, Tsuchiyama A, Imae N, Kurosawa K, Nakamura AM, Ogawa K, Sugita S, Morota T, Honda R, Kameda S, Tatsumi E, Cho Y, Yoshioka K, Yokota Y, Hayakawa M, Matsuoka M, Sakatani N, Yamada M, Kouyama T, Suzuki H, Honda C, Yoshimitsu T, Kubota T, Demura H, Yada T, Nishimura M, Yogata K, Nakato A, Yoshitake M, Suzuki AI, Furuya S, Hatakeda K, Miyazaki A, Kumagai K, Okada T, Abe M, Usui T, Ireland TR, Fujimoto M, Yamada T, Arakawa M, Connolly HC Jr, Fujii A, Hasegawa S, Hirata N, Hirata N, Hirose C, Hosoda S, Iijima Y, Ikeda H, Ishiguro M, Ishihara Y, Iwata T, Kikuchi S, Kitazato K, Lauretta DS, Libourel G, Marty B, Matsumoto K, Michikami T, Mimasu Y, Miura A, Mori O, Nakamura-Messenger K, Namiki N, Nguyen AN, Nittler LR, Noda H, Noguchi R, Ogawa N, Ono G, Ozaki M, Senshu H, Shimada T, Shimaki T, Shirai K, Soldini S, Takahashi T, Takei Y, Takeuchi H, Tsukizaki R, Wada K, Yamamoto Y, Yoshikawa K, Yumoto K, Zolensky ME, Nakazawa S, Terui F, Tanaka S, Saiki T, Yoshikawa M, Watanabe S, Tsuda Y (2022) Pebbles and sands on asteroid (162173) Ryugu: on-site observation and returned particles from two landing sites. *Science* 375:1011–1016. <https://doi.org/10.1126/science.abj8624>
- Tsuda Y, Saiki T, Terui F, Nakazawa S, Yoshikawa M, Watanabe S, Hayabusa2 Project Team (2020) Hayabusa2 mission status: landing, roving and cratering on asteroid Ryugu. *Acta Astronaut* 171:42–54. <https://doi.org/10.1016/j.actaastro.2020.02.035>
- Yada T, Abe M, Okada T, Nakato A, Yogata K, Miyazaki A, Hatakeda K, Kumagai K, Nishimura M, Hitomi Y, Soejima H, Yoshitake M, Iwamae A, Furuya S, Uesugi M, Karouji Y, Usui T, Hayashi T, Yamamoto D, Fukai R, Sugita S, Cho Y, Yumoto K, Yabe Y, Bibring JP, Pilorget C, Hamm V, Brunetto R, Riu L, Lourit L, Loizeau D, Lequertier G, Moussi-Soffys A, Tachibana S, Sawada H, Okazaki R, Takano Y, Sakamoto K, Miura YN, Yano H, Ireland TR, Yamada T, Fujimoto M, Kitazato K, Namiki N, Arakawa M, Hirata N, Yurimoto H, Nakamura T, Noguchi T, Yabuta H, Naraoka H, Ito M, Nakamura E, Uesugi K, Kobayashi K, Michikami T, Kikuchi H, Hirata N, Ishihara Y, Matsumoto K, Noda H, Noguchi R, Shimaki Y, Shirai K, Ogawa K, Wada K, Senshu H, Yamamoto Y, Morota T, Honda R, Honda C, Yokota Y, Matsuoka M, Sakatani N, Tatsumi E, Miura A, Yamada M, Fujii A, Hirose C, Hosoda S, Ikeda H, Iwata T, Kikuchi S, Mimasu Y, Mori O, Ogawa N, Ono G, Shimada T, Soldini S, Takahashi T, Takei Y, Takeuchi H, Tsukizaki R, Yoshikawa K, Terui F, Nakazawa S, Tanaka S, Saiki T, Yoshikawa M, Watanabe S, Tsuda Y (2022) Preliminary analysis of the Hayabusa2 samples returned from C-type asteroid Ryugu. *Nat Astron* 6:214–220. <https://doi.org/10.1038/s41550-021-01550-6>
- Yumoto K, Cho Y, Yabe Y, Mori S, Ogura A, Miyazaki A, Yada T, Hatakeda K, Yogata K, Abe M, Okada T, Nishimura M, Usui T, Sugita S (2022) Visible multi-band spectra and specular reflectivity of Ryugu returned samples. In: Abstracts of the 53th lunar and planetary science conference, Woodlands, Texas, 7–11 March 2022.

Publisher's Note

Springer Nature remains neutral with regard to jurisdictional claims in published maps and institutional affiliations.

Submit your manuscript to a SpringerOpen[®] journal and benefit from:

- Convenient online submission
- Rigorous peer review
- Open access: articles freely available online
- High visibility within the field
- Retaining the copyright to your article

Submit your next manuscript at ► [springeropen.com](https://www.springeropen.com)